AER870: AEROSPACE ENGINEERING THESIS
DEPARTMENT OF AEROSPACE ENGINEERING
RYERSON UNIVERSITY
350 VICTORIA ST. TORONTO, ONTARIO, M5B 2K3

Cubesat BDOT Control Modelling- Detumbling and Angular Momentum Management

Veronica Chigoziri Obodozie

AER870(1): Aerospace Engineering Thesis
Dr. Anton De Ruiter
Ryerson University
Winter 2020

1 Acknowledgements

The author would like to thank her faculty advisor Dr de Ruiter, for the opportunity to work on this project and his guidance and advice throughout this project. Additionally, the author would also like to show appreciation to Mike Alger and William Travis for generously giving their time and knowledge assisting in the explanation of the concepts and models which laid the foundation for this project as well as improvement suggestions. The author would like to thank her parents and siblings for their support and encouragement throughout her undergraduate career. Especially Maria-Regina and Michael Obodozie for their assistance in keeping the thesis progress on schedule and for proofreading the final report.

2 Abstract

The purpose of this thesis is to explore the uses of magnetic torquers on a CubeSat. This is focused on tuning the gain value of a B-DOT controller for the Detumbling of the ESSENCE CubeSat. This was tested with a converged rate value of $0.05 deg/secs$ as the criterion over 15 orbits; with each simulation having a total of 20 runs. The matrix chosen for the gain value was tested to ensure it was feasible regardless of a change in the initial tumbling rate, settling time and slight command errors. The Appendix shows sample test results for this model. The second magnetic torquer use which was to have a gain tuning was the momentum dumping. the control law was a variant of the B-DOT controller focusing on the angular momentum, this was applied to the form of Angular Momentum Management of the CubeSat. Although the overall testing procedure was edited, more tuning is required for the momentum dumping gain value.

Contents

Nomenclature

Acronyms

$ADCS$ Attitude Determination and Control System

$DESCENT$ DEorbiting SpaceCraft using ElectrodyNamic Tethers

$ESSENCE$ Educational Space Science and Engineering CubeSat Experimental Mission

ISS International Space Station

LEO Lower Earth Orbit

WBS Work Breakdown Structure

List of Symbols Greek

ω Angular Velocity

ξ_m Inclination of spacecraft orbit relative to geomagnetic eqautorial plane

Other Symbols

$\dot{B}$ Rate of Change of Magnetic Field

T_{orb} Orbital Period

J_{min} Minimum principal moment of inertia

List of Symbols Alphanumeric

$\widetilde{m}$ Ideal Magnetic Moment Dipole

b Geomagnetic Field

L Control Torque Perpendicular to B

m_{cmd} Commanded Magnetic Moment Dipole

B Magnetic Field sensed by magnetometers

k B-DOT Scalar Gain

m Magnetic Dipole

$\mathbf{h}$ wheel angular momentum

Vectors and Matrices

I_3 A three by three identity matrix

List of Figures

List of Tables

3 Introduction

3.1 Purpose

The purpose of this document is to summarize the progress of the thesis. This will include a brief description of the project, results obtained. In addition the development plan is presented, describing the team progress up to completion.

3.2 Mission Overview ESSENCE

Aiding the development and launch of the Educational Space Science and Engineering CubeSat Experimental Mission (ESSENCE) where novel attitude control theories for spacecrafts. This will be a 2U CubeSat designed built and launched from the International Space Station (ISS) [3]. This project is a subgroup of the Attitude Determination and Control System (ADCS) team, specifically working with the magnetic torquers. As the previous mission DEorbiting SpaceCraft using ElectrodyNamic Tethers (DESCENT) has been developed and is awaiting launch, it will provide a base model and guidance on how to complete the project.

The primary goal of this project is to model and simulate the detumbling and reaction wheel momentum dumping using the magnetic torquers of the CubeSat. The bulk of the mission will be achieved using the B-DOT control law, Appendix A explains this in more detail. A secondary goal of the mission will be the alignment of the spacecraft with the magnetic field of the Earth. This shall be achieved by finding the constant moment vector to apply to the CubeSat to keep it properly oriented.

The ESSENCE mission requirement document specifies in $REQ-M-PER-001$ that the CubeSat should detumble within 24 hours and switch to coarse pointing with magnetic torquers [4]. Although this was not directly considered in this report it is a useful requirement for the overall mission.

4 Magnetic Torquers Use

4.1 B-DOT Controller Detumbling

The primary task of this project was to establish a suitable gain value applied to the BDOT control law in order to detumble the CubeSat. The major difference between ESSENCE and DESCENT ADCS which has an impact on the overall thesis project is the addition of three reaction wheels. In the case of detumbling this difference does not affect much as the reaction wheels during this stage are inactive.

4.1.1 Detumbling BDOT Controller.

As DESCENT uses a similar control law, the field controller created by William Travis[2] for the mission was utilized. This is a magnetic the rate only dampening controller which slows rate for more precise estimator and control law. To save power the magnetic moment applied is orthogonal to the measured magnetic field. This is the first law used in the project which relates the CubeSat attitude rates to the magnetic field measured by the magnetometers.

$$\vec{m_{cmd}} = K_{BDOT}\dot{b} \tag{1}$$

For a more in-depth explanation of this law, Appendix a is available. This states that the magnetic controller commanded dipole moment is equal to the magnetic field time derivative scaled by a constant gain matrix [5]. As the maximum moment dipole for each axis of the CubeSat is known to be:

$$\begin{aligned} X_B &= 0.06Am^2 \\ Y_B &= 0.12Am^2 \\ Z_B &= Y_B \end{aligned}$$

These values can be related to the axis defined in 4.1

Figure 4.1: ESSENCE Dipole axis Definition

The gain matrix is used to scale these accordingly. Which is given by:

$$\begin{bmatrix} k_{bdot,x} & 0 & 0 \\ 0 & k_{bdot,y} & 0 \\ 0 & 0 & k_{bdot,z} \end{bmatrix}$$

This matrix was chosen for its flexibility in performance. From figure 4.1, the roll axis is the longest, meaning the torque needs to be a little stronger to slow down at the same rate. Ignoring residual dipole and internal currents, the minimum dipole would be zero.

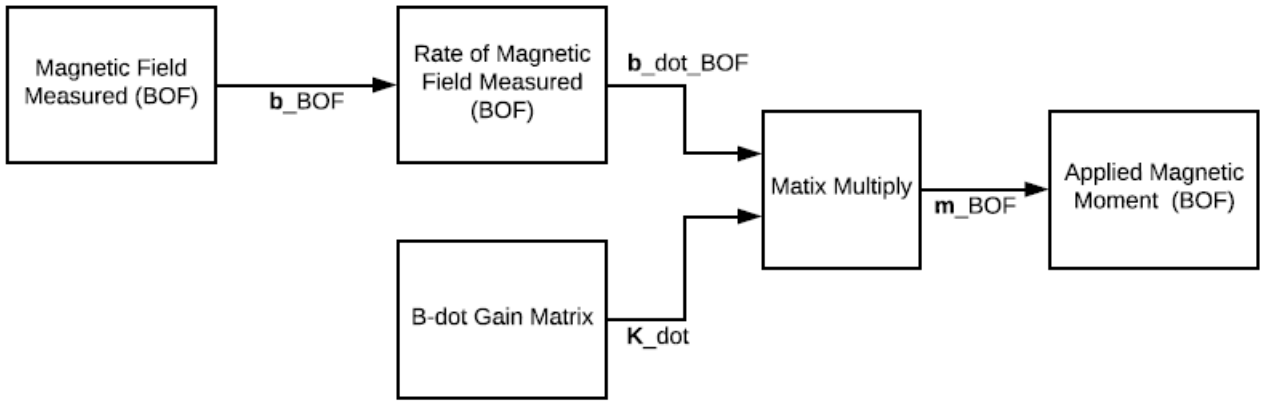

Figure 4.2: DESCENT BDOT Controller Block Diagram[2]

Figure 4.2 shows the block diagram for the DESCENT BDOT controller. The measured magnetic field is used to calculate the rate of change of the magnetic field by performing a discrete time derivative:

$$\dot{b}_k = \frac{b_k - b_{k-1}}{t_k - t_{k-1}} \tag{2}$$

The this rate is then multiplied by a constant gain matrix to compute the commanded magnetic moment; this is given in the body frame. This is currently being updated to include a low-pass filter for the magnetic field rate of change, with the effort of reducing noise.

4.2 Momentum Dumping

The introduction of reaction wheels is one of the key differences between DESCENT and ESSENCE projects. The overview being the second control law in this project shall be a modified BDOT control which utilises the reaction wheel speed. The major difference between DESCENT and ESSENCE in terms of this project are the three reaction wheels that have been added. As such a control law to command a magnetic dipole moment for momentum dumping through BDOT control will also be utilised.

$$\vec{m} = \frac{k}{\left\|\vec{B}\right\|}\vec{h} \times \vec{b} \tag{3}$$

This can be compared to the control law described by equation 10, as the angular velocity of the spacecraft has been replaced with the angular momentum of the wheels. From this it can be observed that no torque can be exerted when the wheel angular momentum and B are zero.

5 Simulation Software

In this section the simulation software used for testing shall be explained. Primarily MATLAB and SIMULINK were used to model the B-DOT controller.

5.1 Detumbling Model

As testing for the gain matrix is primarily done using a B-DOT controller Simulink model created by Mike Alger, a breakdown f this model shall be performed. Figure 5.1 below shows the overall Simulink model for the BDOT control test.

This block contains processes which show how the magnetic field is computed,

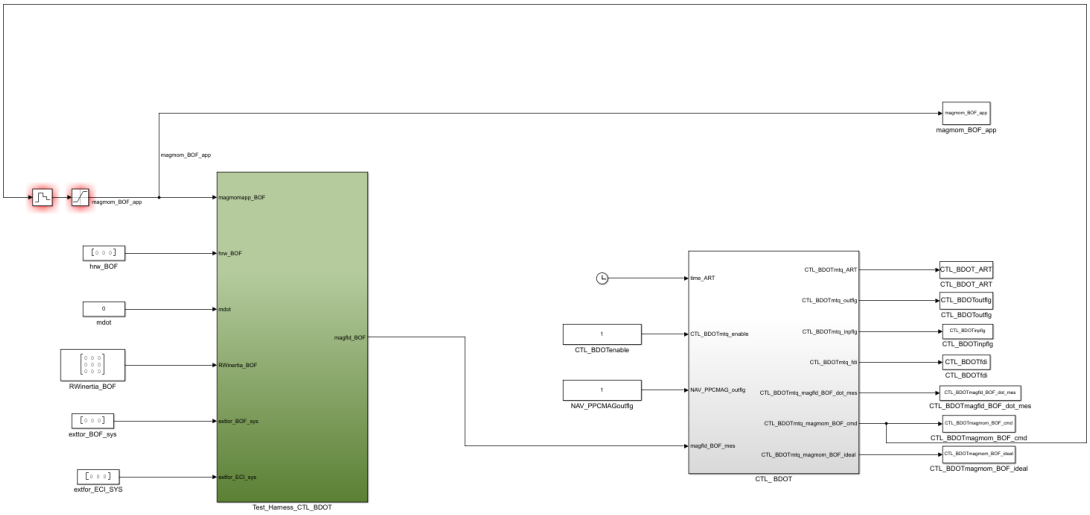

Figure 5.1: TST_CTL_BDOT Model

and outputs the magnetic moment in body frame.

The controller is used to compute commands in the ORB frame for the magnetic controller to execute.This section uses the TST_CTLBDOT model to explain how B-DOT is computed and how the magnetic moment dipole command is estimated.

The overall B-DOT controller model test is shown in Figure 5.2. The input and Outputs of the BDOT controller are listed as follows:

INPUTS

- time_ART Simulation time
- CTL_BDOTTenable: Flag ensuring CTL_BDOT is activated.

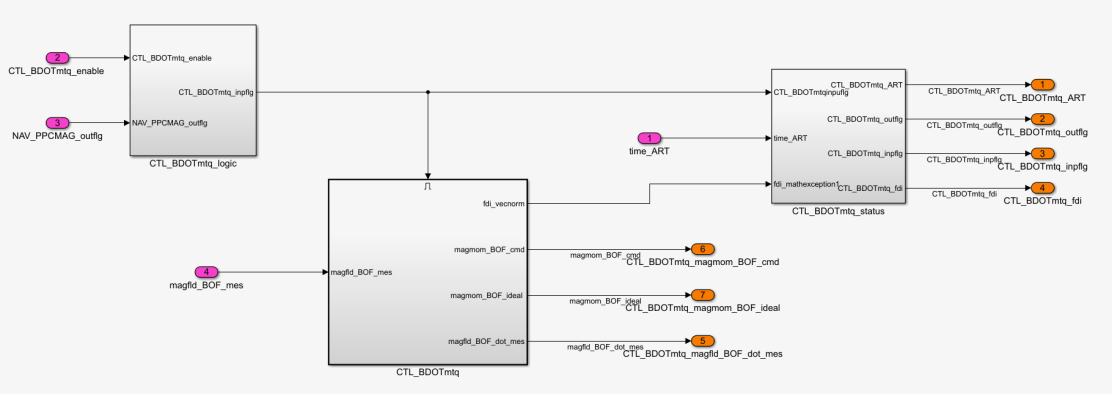

Figure 5.2: BDOT Controller Model

- NAV_PPCMAGoutflg: Flag ensuring correct output.
- Magfld_BOF_mes: Measured magnetic field expressed in the body frame.

OUTPUTS

- CTL_BDOT_ART: Time elapsed during test.
- CTL_BDOToutflg: Flag ensuring CTL_outflg ran correctly.
- CTL_BDOTinpflg: Flag ensuring all before CTL_BDOT ran correctly.
- CTL_BDOTfdi: Flag notifying a math error ocured and data is valid.
- CTL_BDOTmagmom_cmd: Commanded magnetic moment from the controller expressed in the Body frame.
- CTL_BDOTmagmom_ideal: ideal magnetic moment from the controller expressed in the BOF.

Within this block B-DOT gain controller block and the magnetic moment and rate of change of the magnetic field.
Figure 5.3 CTL_BDOTmtq shows how the rate of change of the magnetic field and magnetic moment are computed. This is computed using a Discrete-time derivative of the measured magnetic field with the initial input being zero. The *computeBDOT* function then calculates the magnetic moment by applying the control law as follows:

$$m = \frac{k}{\|B\|}\dot{b} \tag{4}$$

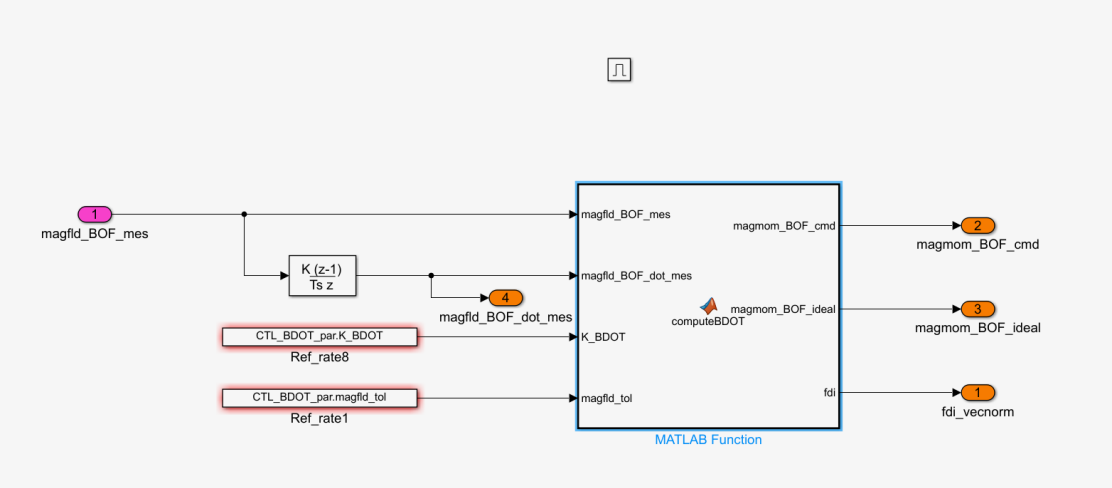

Figure 5.3: BDOT Computation Model

Equation 10 is the general control law being used in this controller. It gives a general magnetic dipole moment (m) relationship between the gain values (k) and measured magnetic field (B).

$$\dot{B} = \frac{b_k - b_{k-1}}{t_k - t_{k-1}} \tag{5}$$

Equation 5 shows how the rate of change is calculated as

$$\widetilde{m} = K_{bdot} \times \dot{B} \tag{6}$$

$$m_{cmd} = (I_{3\times 3} - \frac{bb^T}{\left\|\vec{B}\right\|^2}) \times \widetilde{m} \tag{7}$$

Equations 6 and 7 show how the ideal and commanded magnetic moment are respectively calculated. These are both expressed in the body frame when outputted. Initially the parallel simulation method was used to perform simulations on MATLAB in parallel using the $parfor$ loop. This was a property duplicated from the B-DOT DESCENT code that ESSENCE B-DOT is based on. To save overall computation time a simple for loop was used for individual simulation runs.

5.2 Angular Momentum Management

This model was scheduled for creation later in the project, however with an existing model by William Travis and Mike Alger the test shall be explained. The reaction

wheel test follows a similar structure as the detumbling model.

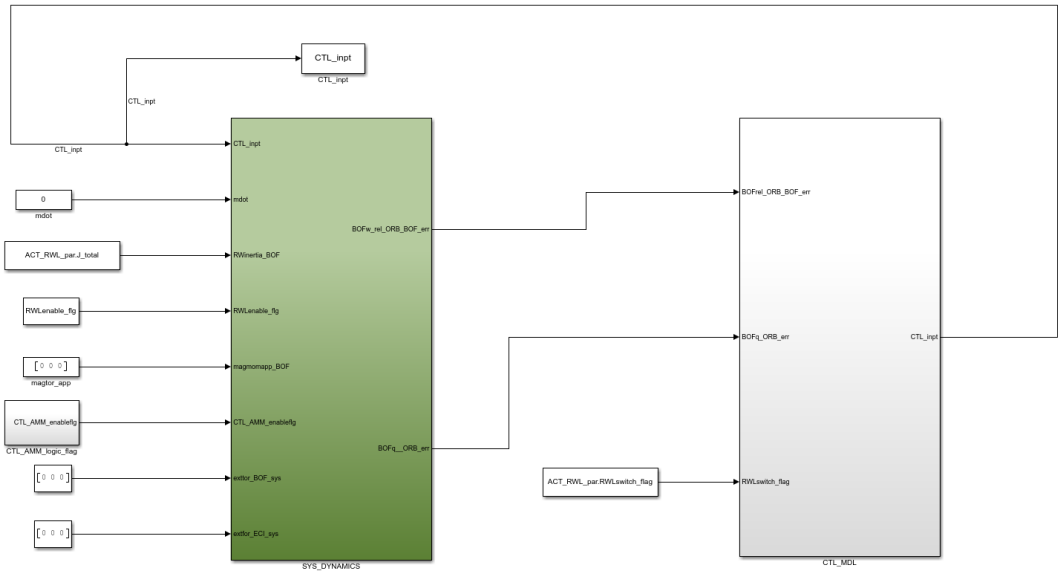

Figure 5.4: Three Wheel Angular Momentum Management Model

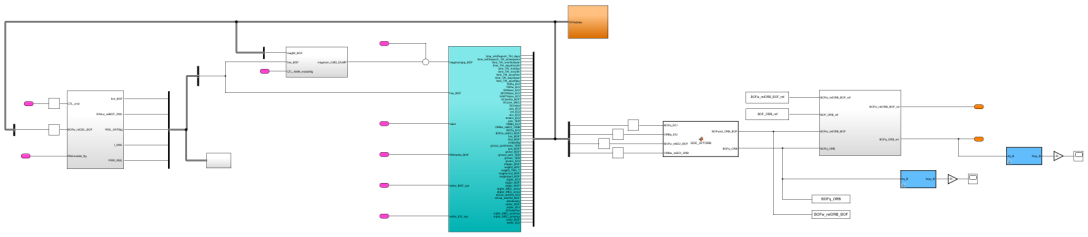

Figure 5.5: System Dynamics Model

Taking a closer look into the system Dynamics test harness model, the Angular Momentum Management control block consisting of the momentum dumping test model can be found.

The momentum dumping gain is the main parameter being tested. Currently it is set at half of the maximum CubeSat inertial in the body frame. The model shown in figure 5.7. The relevant output of the simulation is the magnetic torquer voltage, with its maximum set at 3.3 volts.

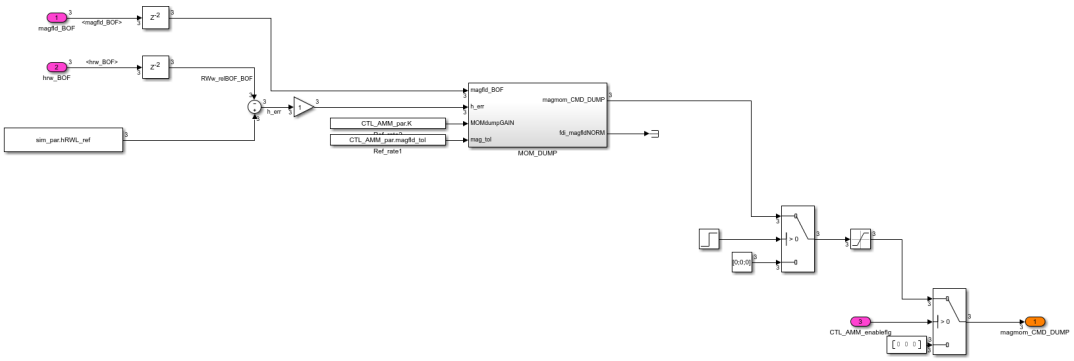

Figure 5.6: Angular Momentum Management Control Block

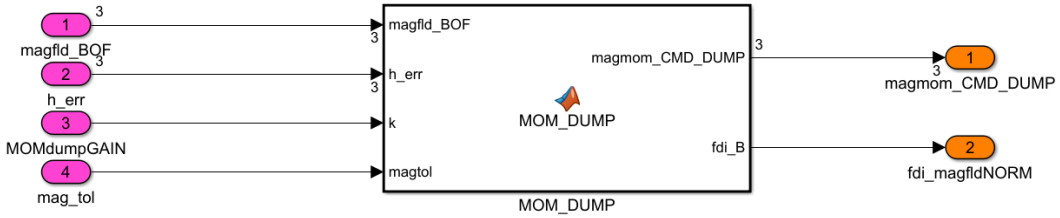

Figure 5.7: Momentum Dumping Model

6 Results

6.1 B-DOT Controller Gain

This section focuses on what has been achieved at this point of the project, highlighting how this was done as well as the results. Due to the nature of this aspect of the project, the optimum B-DOT gain value was determined through trial and error.

6.1.1 Methodology

As explained previously the gain matrix is determined through scaling the spacecraft inertial control by a factor. This method was chosen over using direct factors to allow flexibility in performance; as the detumbling rates of each axis is approximately the same. Meaning the Roll axis has a stronger torque due to its length difference. The following gain factors and ranges shall be utilised in this project:

Table 6.1: Gain Factor and Range per Axis

Gain Factor	**X-range** $\times 10^3$		**Y-range** $\times 10^3$		**Z-range** $\times 10^3$	
	Min	Max	Min	Max	Min	Max
10	1.3575	1.64	0.300	0.362	0.294	0.355
40	5.4299	6.5599	1.200	1.4497	1.1753	1.4199
50	6.7873	8.1998	1.500	1.8122	1.4691	1.7749
60	8.1448	9.8398	1.800	2.1746	1.763	2.1299
70	9.5023	11.48	2.100	2.537	2.0568	2.4848
100	13.575	16.40	3.000	3.6243	2.9383	3.5498
250	33.937	40.999	7.500	9.0608	7.3457	8.8745

Table 6.1 shows the gain ranges per axis; it should be noted that for each run the gain factor increases by a factor of 1.01.
$GainMatrix = Gainfactor \times I$

The settled angular rate tolerance of 0.05 deg/sec was placed, with a max dipole of 0.03 Am^2 single panel per axis. K_BDOT was the main focus. Test simulations that are within the tolerance level pass. Based on this criterion the gain matrix that produces the least number of failed cases shall be utilized. Each simulation has 20 sets with a length of 15 orbits. According to the interface Definition Document of the NanoRacks CubeSat deployer, the tip-off rate upon deployment is 5 $deg/second$ [6]. Initial tests were conducted by varying the following parameters:

- Gain Factor
- Expected Settling Time
- Initial Tumblimg Rate.

6.1.2 Gain Factor Variation Relationship

With estimated settling of 9 orbits (50013 seconds) and an initial tumbling rate of 5 $deg/secs$ the gain factor was varied. Table 6.2 shows the relationship between the gain factor and the number of passed runs per simulation. By keeping all other parameters constant it can be seen that at extremely low and high factors, like 10 and 250, there are no runs which pass the criterion. Focussing on the gain factors with the highest number of criterion successes 40 and 50 shall be the main focus for the rest of the project.

Table 6.2: Gain Factor Variation Relationship

Gain Factor Value	**Initial Tumbling rate (deg/s)**	**Detumbling Time (s)**	**Number of Passes (/20)**
10	5	50013	0
40	5	50013	15
50	5	50013	13
60	5	50013	8
70	5	50013	2
100	5	50013	0
250	5	50013	0

6.1.3 Expected Settling Time Variation Relationship

In the simulator, the settling times are estimated by orbits; for this portion of the analysis these can be viewed as the detumbling times. The initial detumbling rate of 5 $deg/secs$ was used for all simulation trials.

Table 6.3 shows the number of successful runs for the estimated settling orbits of

Table 6.3: Settling Time Variation Relationship

Gain Factor Value	**Initial Tumbling rate (deg/s)**	**Detumbling Time (s)**	**Number of Passes (/20)**
40	5	33342	1
50	5	33342	5
40	5	50013	15
50	5	50013	13
40	5	55569	16
50	5	55569	14

6, 9, and 10 respectively. For a simulation length of 15 orbits the settling estimate shows a somewhat linear relationship, the longer the time the more successful runs a simulation has. A discrepancy in the overall trend of a higher success rate at a gain factor of 40 than at 50 is shown when the settling time is reduced to 6 orbits. It can be inferred that the larger gain factor takes less time to settle, so although it has a lower success rate in general at 6 orbits some of its runs pass the criterion.

6.1.4 Initial Tumbling Rate Variation Relationship

In this section the initial tumbling rate of the CubeSat is considered with an estimated settling length of 9 orbits. The aim is not only to show how the initial

tumbling rate affects the simulation,but to prove the gain factor chosen can perform regardless of discrepancies in estimated tip off rate [6].

Table 6.4: Tumbling Rate Variation Relationship

Gain Factor Value	**Initial Tumbling rate (deg/s)**	**Detumbling Time (s)**	**Number of Passes (/20)**
40	1	50013	11
50	1	50013	16
60	1	50013	10
100	1	50013	0
40	3	50013	10
50	3	50013	13
60	3	50013	11
40	5	50013	15
50	5	50013	13
60	5	50013	8
100	5	50013	0
40	6	50013	14
50	6	50013	14
60	6	50013	7
100	6	50013	0

Table 6.4 and Figure 6.1 illustrate the success rate for simulations of varying initial tumbling rates and gain factor. Although this relationship cannot be assumed linear, it shows a trend. With the gain factor of 40 having the most unpredictable variations decreasing in success rates.

The gain factor of 60, although a clear trend is shown with its success rates continuously deceasing past an initial rate of 3 deg/secs has demonstrated an overall low success rate. Overall the gain factor of 50 showed near consistent success rates below and above the rated Nanoracks tip-off rates.

6.1.5 Final B-dot Controller Gain Matrix Validation

Ultimately, the gain factor of 50 was chosen for final evaluation due to overall consistency and limited response to changes. Table 6.5 shows the simulation data for the B-DOT gain testing, these parameters account for any variation between

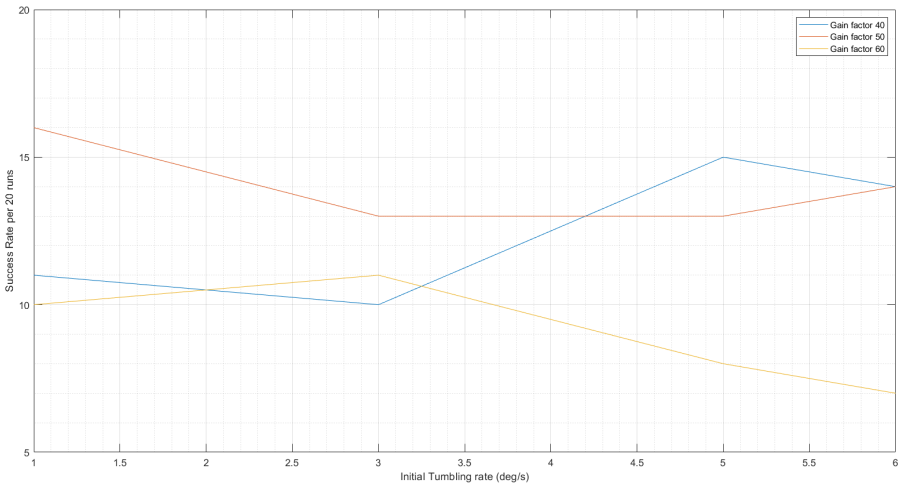

Figure 6.1: Graph of Tumbling vs Success Rate.

real world and simulation.

Table 6.5: Summary of Simulation Data for Gain Selection

Gain Factor Value	**Initial Tumbling rate (deg/s)**	**Detumbling Time (s)**	**Number of Passes (/20)**
50	5	55569	13

The successful runs per simulations were compiled and outlined in table B.1 of Appendix B. Based on this list, runs which were successful in various conditions were chosen. Table 6.6 shows the settle time maximum torque and gain matrix associated with each run.

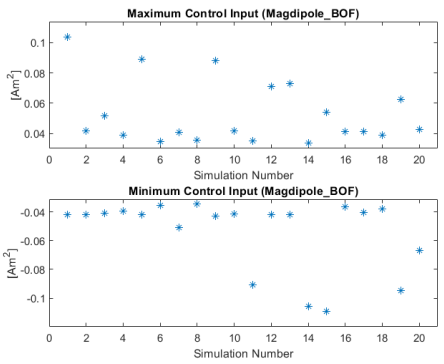

(a) Maximum Control Input Plot for Set of Simulations

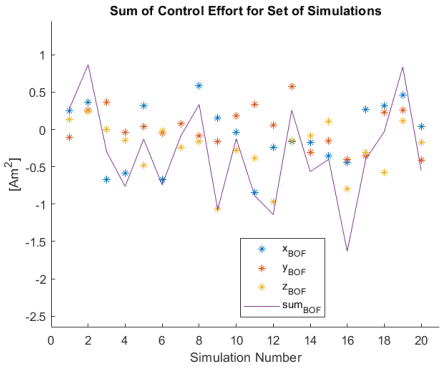

(b) Sum of Control Effort for Set of Simulations

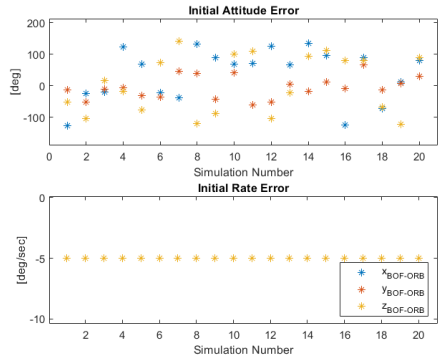

(c) Initial Attitude and Rate Error Plot for Set of Simulations

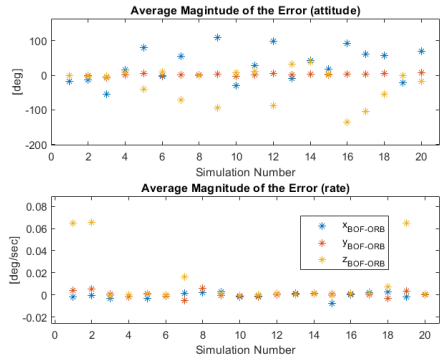

(d) Average Magnitude of the Error Plot for Set of Simulations

Figure 6.2: Final Simulation Summary Plots

Table 6.6: Simulation Run Results

Run	Settle Time	Maximum Torque ($\times 10^{-6} nm$)	Gain Matrix ($\times 10^3$)
6	55569	1.351	$\begin{bmatrix} 7.1336 & 0 & 0 \\ 0 & 1.5765 & 0 \\ 0 & 0 & 1.5441 \end{bmatrix}$
11	55569	1.428	$\begin{bmatrix} 7.4974 & 0 & 0 \\ 0 & 1.6569 & 0 \\ 0 & 0 & 1.6229 \end{bmatrix}$
16	55569	1.413	$\begin{bmatrix} 7.8799 & 0 & 0 \\ 0 & 1.7415 & 0 \\ 0 & 0 & 1.7056 \end{bmatrix}$
20	55569	1.476	$\begin{bmatrix} 8.1998 & 0 & 0 \\ 0 & 1.8122 & 0 \\ 0 & 0 & 1.7749 \end{bmatrix}$

The gain matrix from run 16 was chosen as the final gain matrix for the ESSENCE B-DOT controller. Overall, higher gain values require higher sample rates.

$$\begin{bmatrix} 7.8799 & 0 & 0 \\ 0 & 1.7415 & 0 \\ 0 & 0 & 1.7056 \end{bmatrix} \tag{8}$$

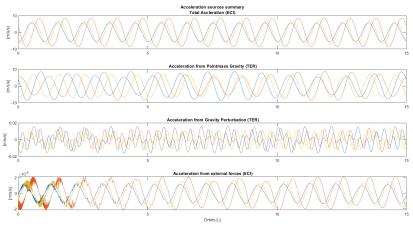

(a) Acceleration Sources Summary

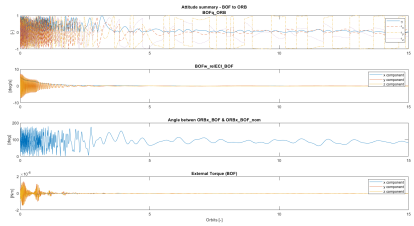

(b) Attitude Summary BOF to ORB

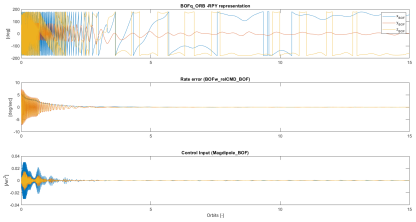

(c) Controller Error and Control Input

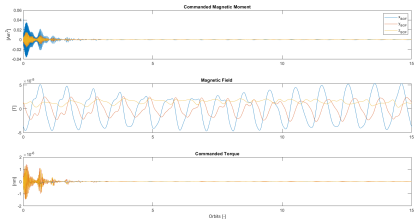

(d) Magnetic Moment Field and Resulting Torque

Figure 6.3: Final Simulation Sample Result run 16 of 20.

6.2 Angular Momentum Management

Following a similar format as the cubesat detumbling test model, a criteria of an RPY and tumbling tolerance of 0.1 *deg* and 0.01 *deg/sec* per axis respectively. Although not much testing could be achieved, the resultant plots are shown below: For a gain value of half of the maximum cubesat inertia, 67.

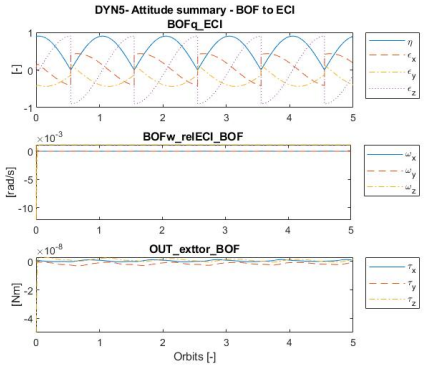

(a) Attitude Summary BOF to ECI

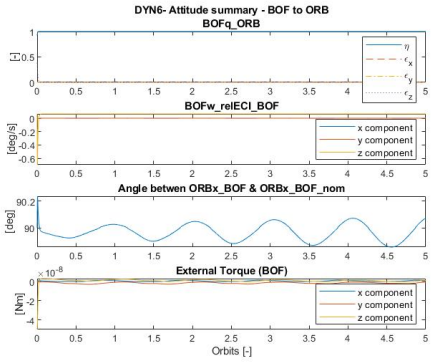

(b) Attitude Summary - BOF to ORB

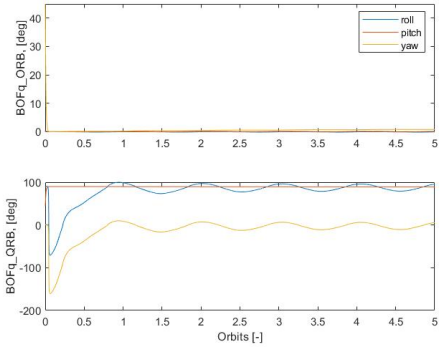

(c) Attitude Summary RPY - ORB

Figure 6.4: Simulation Results for the Momentum Dumping Gain Factor of 0.5.

A gain factor of zero was used when a pattern showing a lack of response to the gain value changes: For a gain value of half of the maximum cubesat inertia, 67.

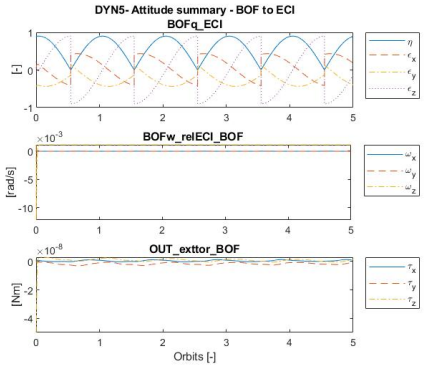

(a) Attitude Summary BOF to ECI

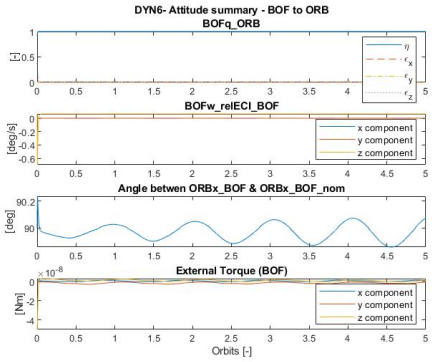

(b) Attitude Summary - BOF to ORB

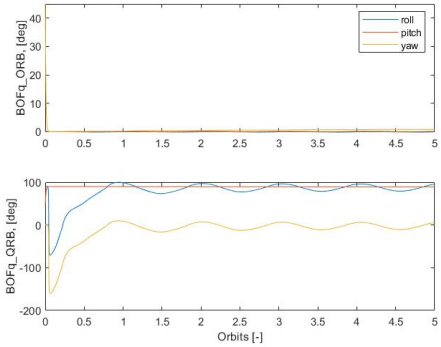

(c) Attitude Summary RPY - ORB

Figure 6.5: Simulation Results for the Momentum Dumping Gain Factor of 0.

More tests and tuning are required for the Angular momentum dumping gain value. As shown in figures 6.4,6.5, there is not much change in the graphs. Additional runs with a factor of 40 and 10 were performed and the results are shown in Appendix C.

7 Conclusion

The main goal of this thesis was to tune a gain value for the B-DOT controller used to detumble the ESSENCE CubeSat through magnetic torquers. Upon reviewing the relationship between the initial tumbling rates, gain factor and estimated settling time initial conditions were set. The initial tumbling rate of $0.5 deg/secs$, settling time of 10 orbits and gain factor of 50. All these were based on the success rates of a 20-run simulation over 15 orbits with an error criterion of $0.05 deg/secs$. Using the final gain matrix shown in equation 8 the B-DOT gain factor was tuned.

In depth testing of the Angular Momentum Management gain factor is required. As much time was spent on trying to understand how the test was created and its relationship with the B-DOT control law, the gain value could not be properly tuned. As such an integrated test between the momentum dumping and detumbling models might be initiated.

8 References

[1] F. Landis Markley and John L. Crassidis. *Fundamentals of Spacecraft Attitude Determination and Control.*, chapter 7.5. Springer Science+Business, 2014.

[2] William Travis. Flight code development and monte-carlo testing of a magnetically actuated attitude control system, 2018.

[3] Mike Alger, Emily Gleeson, and William Travis. Adcs conceptual design essence$_a dcs - tn0 - 003$. Technical report, Educational Space Science and ENgineering CubeSat Experiment Mission (ESSENCE), 2018.

[4] Mike Alger, Emily Gleeson, and William Travis. Adcs requirements definition and preliminary design essence$_a dcs - tno - 002$. Technical report, Educational Space Science and ENgineering CubeSat Experiment Mission (ESSENCE), 2018.

[5] Mike Alger and Emily Glesson. Adcs sw conceptual design document (adcs-sw cdd). Technical report, CubeSat Electrodynamic Tether Deorbit Experiment (CETDE) Mission, 2017.

[6] Tristan Prejean. 4.1.6 deployment velocity and tip-off rate compatibility. Technical report, NanoRacks CubeSat Deployer (NRCSD) Interface Definition Document (IDD), 2018.

A Appendix A: Theory

A.1 BDOT Control Law Theory [1]

This section is heavily influenced by Fundamentals of Spacecraft Attitude Determination and Control. Magnetic Torquers dump excess momentum induced by external disturbances ensuring wheels do not get saturated. Reaction wheels are internal body mechanisms that redistributes spacecrafts angular momentum. These can get saturated from external torques. Other applications include:

- Detumbling
- initial Acquisition
- Precession Control [Change in orientation of rotational axis of a rotating body]
- Nutation Damping
- Momentum Control

Major advantages of the magnetic torquers include their unlimited lifespans, smooth application and absence of catastrophic failure modes. B-DOT control uses the rate of change of the magnetic field. Considering the magnetic field strength decreases as the distance from the Earth increases, due to its inversely proportional relationship to the square of Earth's radius. The torquers are constrained to 2D plane orthogonal to magnetic field.

$$L = m \times b \tag{9}$$

Equation 9 highlights the previous statement by showing the relationship between torque L, magnetic dipole moment m, and the Earths magnetic field b.

DETUMBLING

The control law applied in this section is the Null Angular Velocity control law:

$$m = \frac{k}{\|B\|}\omega \times b \tag{10}$$

This gives the magnetic dipole moment m in terms of the gain value k , the angular velocity ω and the magnetic field which is given by $b = \frac{B}{\|B\|}$. In this control law, the component of the velocity considered is the one perpendicular to the Earth's magnetic field. Using equation 10 to fine-tune the control law:

$$m = -\frac{k}{\|B\|}\dot{B} \tag{11}$$

Where the rate of change of the magnetic field $\dot{B}$ can be modelled in a feedback loop through the moment dipole.

B Appendix B: B-DOT Gain Value Results

B.1 Gain Factor Results.

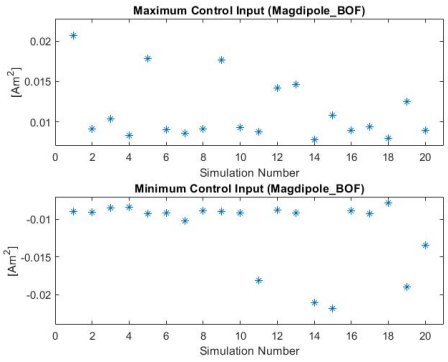

(a) Gain Factor of 10.

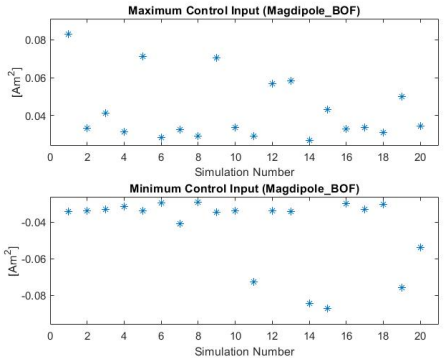

(b) Gain Factor of 40.

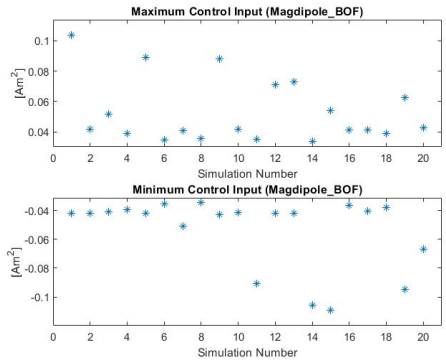

(c) Gain Factor of 50.

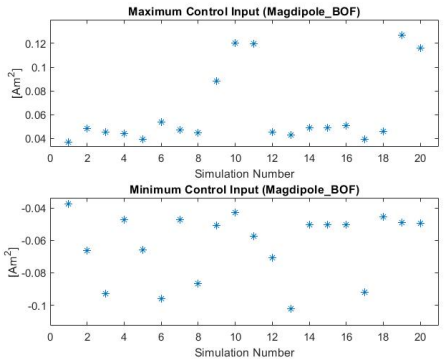

(d) Gain Factor of 60.

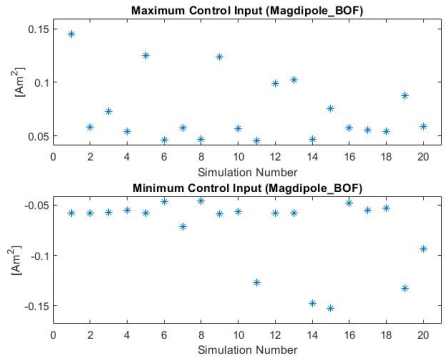

(e) Gain Factor of 70.

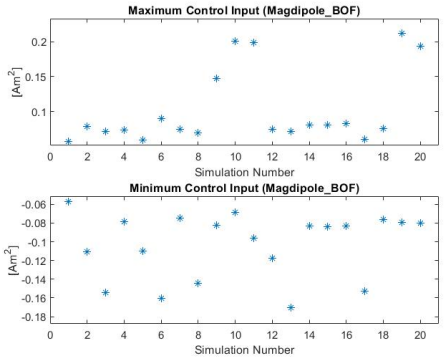

(f) Gain Factor of 100.

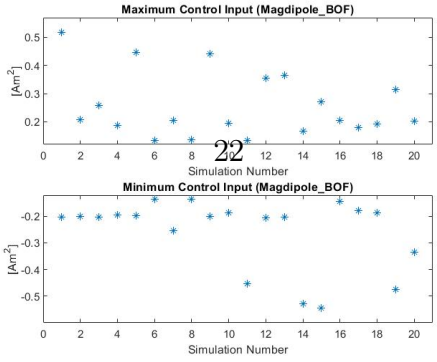

(g) Gain Factor of 250.

Figure B.1: Maximum Control Input Plot for Varying Gain Factor of Simulations

B.2 Initial Tumbling Rate Results.

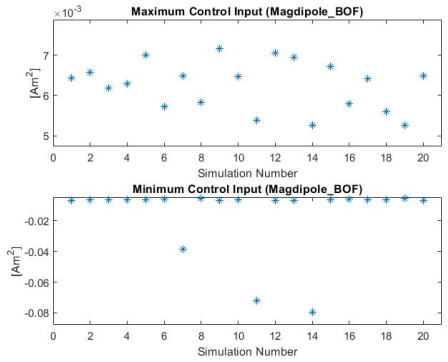

(a) Initial Tumbling rate of 1 deg/sec

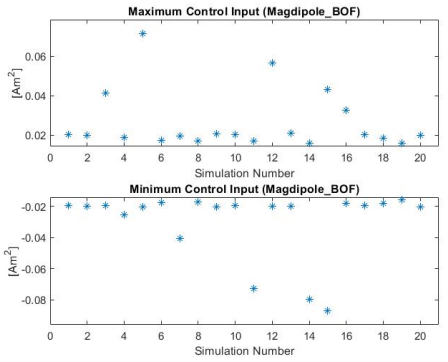

(b) Initial Tumbling rate of 3 deg/sec

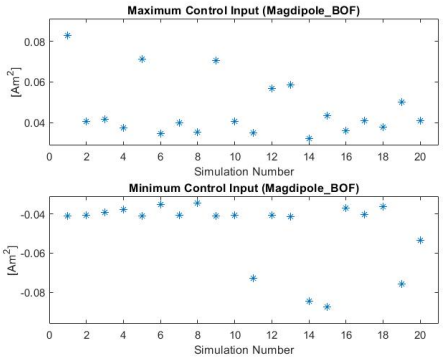

(c) Initial Tumbling rate of 6 deg/sec

Figure B.2: Maximum Control Input Plot for Varying Initial Tumbling Rates of Simulations for Gain Factor of 40 and Settle Time of 9 Orbits.

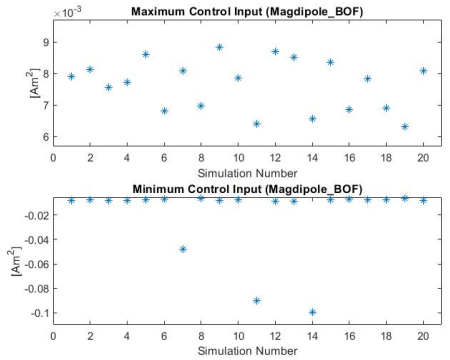

(a) Initial Tumbling rate of 1 deg/sec

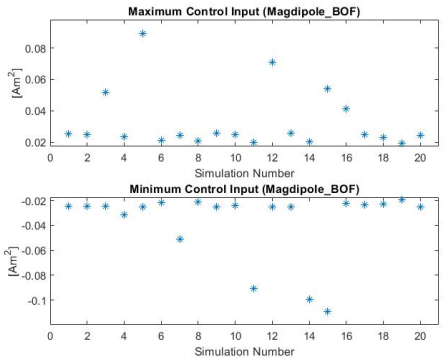

(b) Initial Tumbling rate of 3 deg/sec

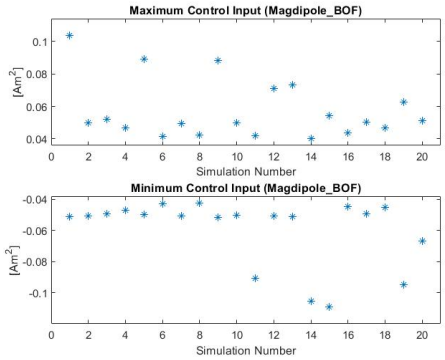

(c) Initial Tumbling rate of 6 deg/sec

Figure B.3: Maximum Control Input Plot for Varying Initial Tumbling Rates of Simulations for Gain Factor of 50 and Settle Time of 9 Orbits.

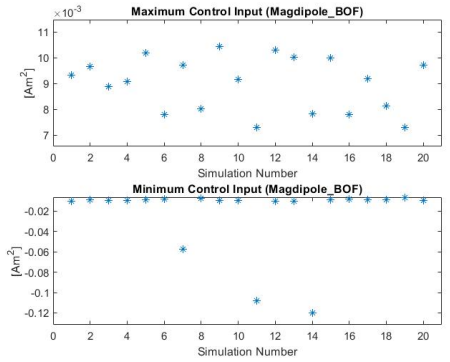

(a) Initial Tumbling rate of 1 deg/sec

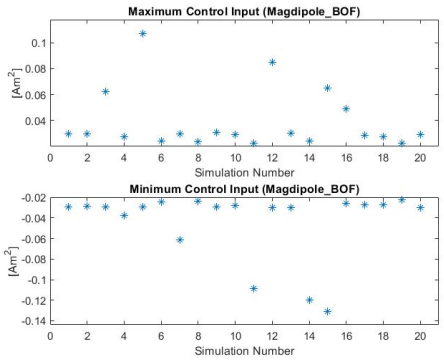

(b) Initial Tumbling rate of 3 deg/sec

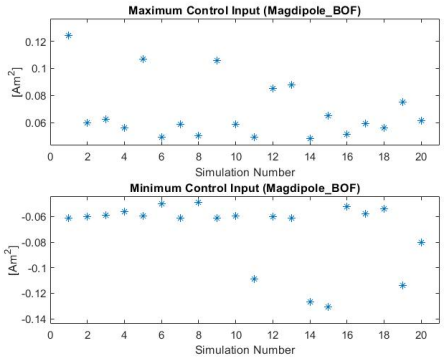

(c) Initial Tumbling rate of 6 deg/sec

Figure B.4: Maximum Control Input Plot for Varying Initial Tumbling Rates of Simulations for Gain Factor of 60 and Settle Time of 9 Orbits.

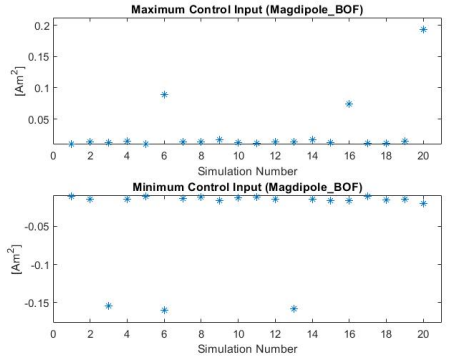

(a) Initial Tumbling rate of 1 deg/sec

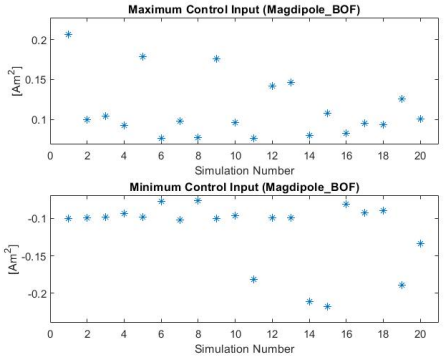

(b) Initial Tumbling rate of 6 deg/sec

Figure B.5: Maximum Control Input Plot for Varying Initial Tumbling Rates of Simulations for Gain Factor of 40 and Settle Time of 9 Orbits.

B.3 Settling Time Results.

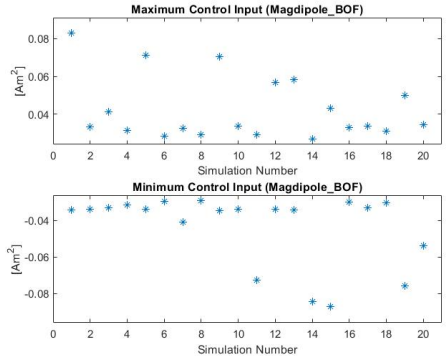

(a) Settle Time of 6 Orbits with a Gain Factor of 40.

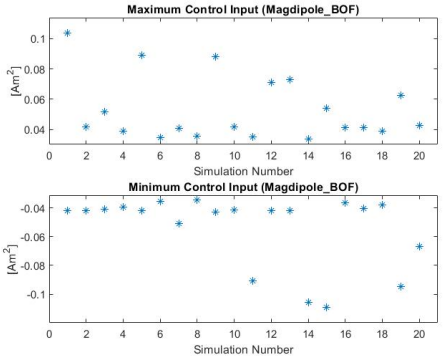

(b) Settle Time of 6 Orbits with a Gain Factor of 50.

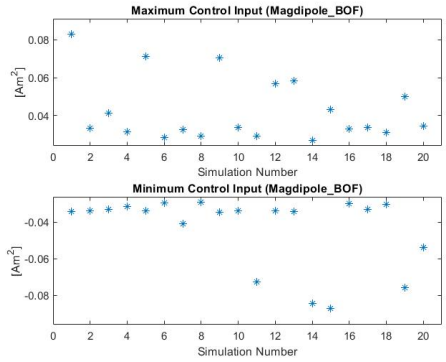

(c) Settle Time of 10 Orbits with a Gain Factor of 40.

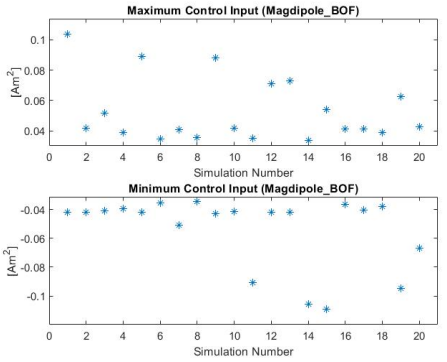

(d) Settle Time of 10 Orbits with a Gain Factor of 50.

Figure B.6: Maximum Control Input Plot for Varying Settling Time of Simulations with Initial Tumbling of 5 deg/sec

B.4 Final B-DOT Gain Value Results.

Table B.1: Successful Run numbers for Gain Factor of 50

Initial Tumbling	Settle Time	Passed runs
1	9	2, 3, 5, 6,7, 9, 10, 11, 12, 13, 15, 16, 17,18, 19, 20
3	9	1, 5, 6, 9, 10, 11, 12, 14, 15, 16, 17, 19, 20
5	9	3, 4, 5, 6, 9, 10, 11, 12, 14, 15,16, 17, 20
6	9	3, 5, 6, 7, 8, 10, 11, 12, 13, 14, 15, 16, 17, 20
5	6	6, 10, 11, 16,17
5	10	3,4, 5, 6, 9, 10, 11, 12,13, 14, 15, 16, 17 20

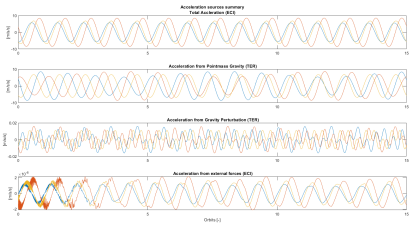

(a) Acceleration Sources Summary

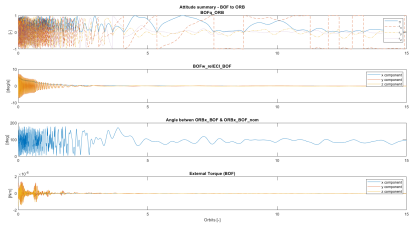

(b) Attitude Summary BOF to ORB

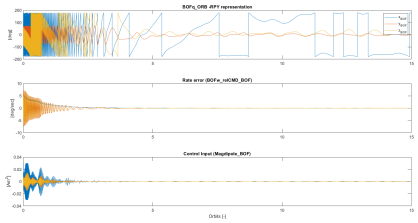

(c) Controller Error and Control Input

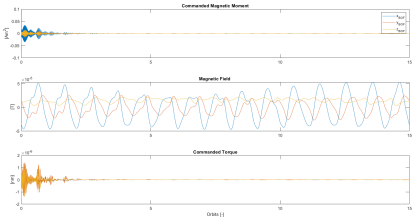

(d) Magnetic Moment Field and Resulting Torque

Figure B.7: Final Simulation Sample Result run 6 of 20.

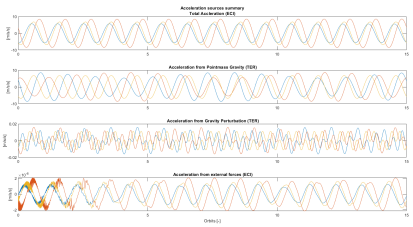

(a) Acceleration Sources Summary

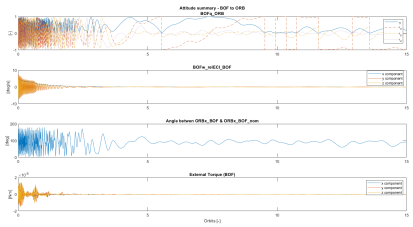

(b) Attitude Summary BOF to ORB

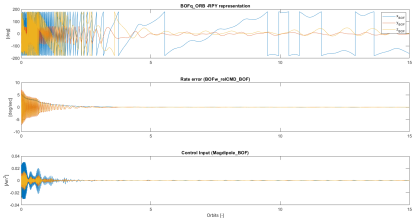

(c) Controller Error and Control Input

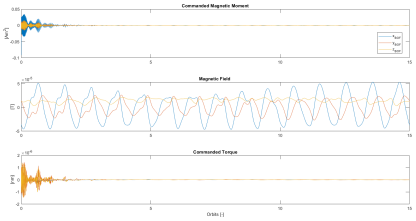

(d) Magnetic Moment Field and Resulting Torque

Figure B.8: Final Simulation Sample Result run 11 of 20.

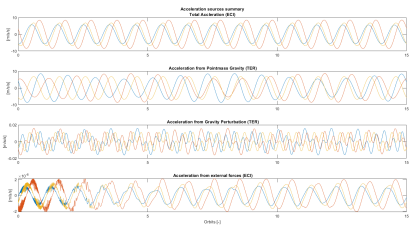

(a) Acceleration Sources Summary

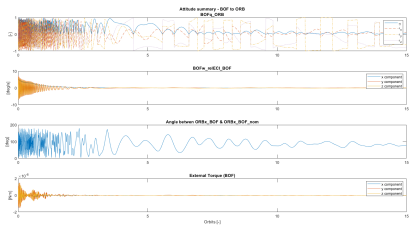

(b) Attitude Summary BOF to ORB

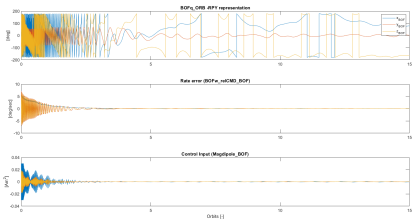

(c) Controller Error and Control Input

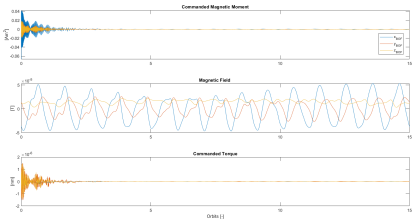

(d) Magnetic Moment Field and Resulting Torque

Figure B.9: Final Simulation Sample Result run 20 of 20.

C Appendix C: Momentum Dumping Simulation Results

This section outlines the results for gain values of 10, 40, 100 times the maximum cubesat inertia, $13575e^3$, $5.4299e^3$, $1.3575e^3$ respectively.

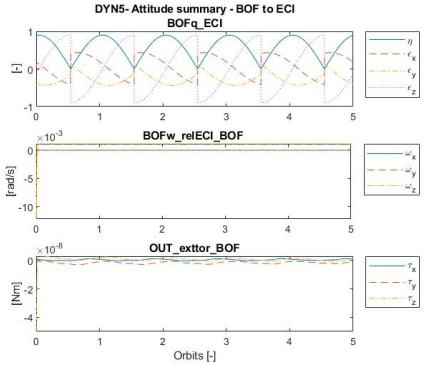

(a) Attitude Summary BOF to ECI

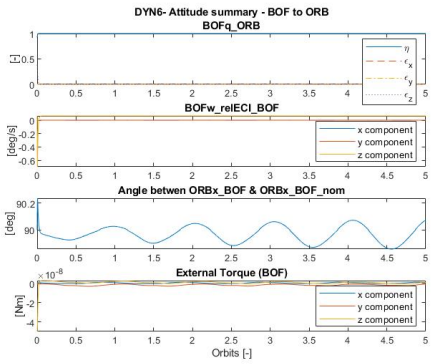

(b) Attitude Summary - BOF to ORB

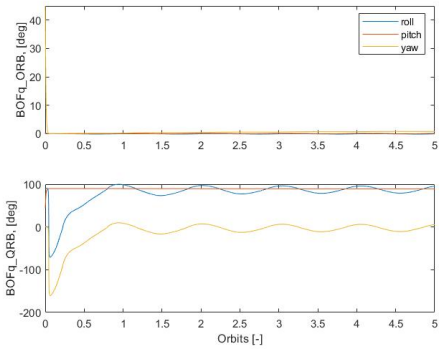

(c) Attitude Summary RPY - ORB

Figure C.1: Simulation Results for the Momentum Dumping Gain Factor of 10.

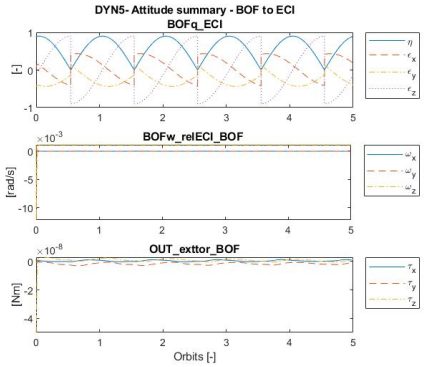

(a) Attitude Summary BOF to ECI

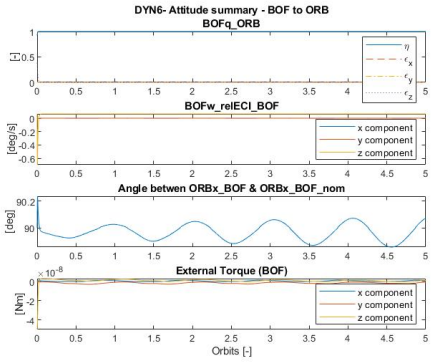

(b) Attitude Summary - BOF to ORB

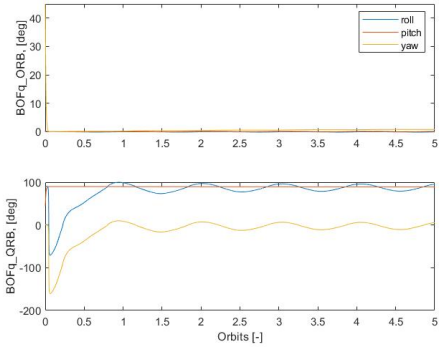

(c) Attitude Summary RPY - ORB

Figure C.2: Simulation Results for the Momentum Dumping Gain Factor of 40.

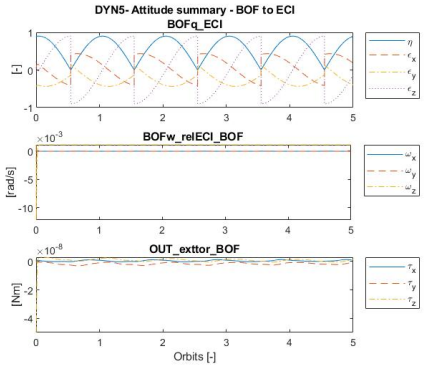

(a) Attitude Summary BOF to ECI

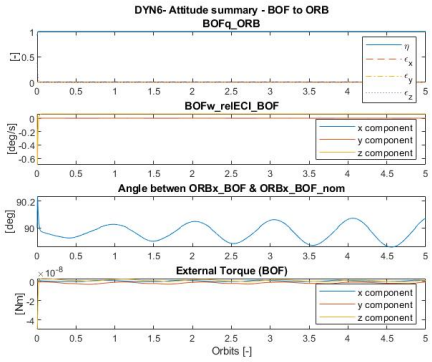

(b) Attitude Summary - BOF to ORB

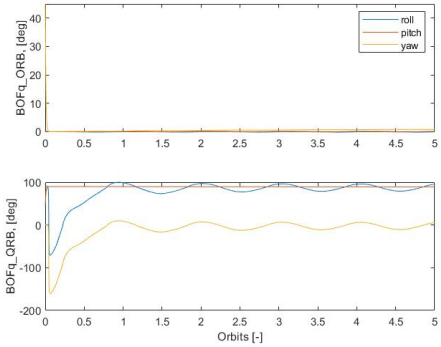

(c) Attitude Summary RPY - ORB

Figure C.3: Simulation Results for the Momentum Dumping Gain Factor of 1000.